

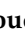



## Article

# Effects of Injection Timing and Antioxidant on NO<sub>x</sub> Reduction of CI Engine Fueled with Algae Biodiesel Blend Using Machine Learning Techniques

Elumalai Perumal Venkatesan <sup>1,\*</sup>, Parthasarathy Murugesan <sup>2</sup>, Sri Veera Venkata Satya Narayana Pichika <sup>3</sup>, Durga Venkatesh Janaki <sup>1</sup>, Yasir Javed <sup>4</sup>, Z. Mahmoud <sup>5,6</sup> and C Ahamed Saleel <sup>7</sup>

<sup>1</sup> Department of Mechanical Engineering, Aditya Engineering College, Surampalem 533437, India

<sup>2</sup> School of Mechanical and Construction, Vel Tech Rangarajan Dr. Sagunthala R&D Institute of Science and Technology, Chennai 600062, India

<sup>3</sup> Department of Mechanical Engineering, BITS-Pilani Hyderabad Campus, Secunderabad 500078, India

<sup>4</sup> Department of Computer Science, College of Computer and Information Sciences, Prince Sultan University, Riyadh 11586, Saudi Arabia

<sup>5</sup> Research Center for Advanced Materials Science (RCAMS), King Khalid University, P.O. Box 9004, Abha 61413, Saudi Arabia

<sup>6</sup> Physics Department, Faculty of Science, King Khalid University, P.O. Box 9004, Abha 61413, Saudi Arabia

<sup>7</sup> Department of Mechanical Engineering, College of Engineering, King Khalid University, Asir-Abha 61421, Saudi Arabia

\* Correspondence: elumalaimech89@gmail.com; Tel.: +91-869-5173-017

**Abstract:** Fossil fuels are depended upon often in the transport sector. The use of diesel engines in all areas produce pollutants, such as NO<sub>x</sub> and CO, which cause serious environmental pollution and hazards, such as global climate change and breathing difficulties. Conventional fuel usage should be reduced, and there should be a shift toward alternative fuels. For compression ignition (CI) engines, microalgae biodiesel has been promoted as a clean, sustainable fuel. This is because it possesses desired traits, such as a quick rate of development, high productivity, and the capacity to turn CO<sub>2</sub> into fuel. When algal biodiesel is used, pollutants, such as CO, UBHC, and smoke, are typically reduced, whereas NO<sub>x</sub> emissions are typically increased. The adoption of an exhaust gas recirculation technology and the advancement or delay of injection timing can effectively reduce NO<sub>x</sub> formation. Incorporating antioxidant chemicals such as butylated hydroxyl anisole (BHA) into fuel also minimizes NO<sub>x</sub> formation. In this study, the use of microalgae biodiesel as a substitute fuel for CI engines was investigated by altering the injection timing and adding each antioxidant in two doses. According to ASTM standard test procedures for biodiesel, the fuel qualities of various blends of algal biodiesel with antioxidants were tested and compared with the diesel fuel. The experiments were conducted using CI engines, and parameters were examined, such UBHC, CO, NO<sub>x</sub>, and smoke opacity. In comparison to diesel fuel, B20 + 30% BHA (21 bTDC) blends produced 49% lower oxides of nitrogen. The smoke, HC, and CO emissions of fuel blend B20 + 30% BHA (25 bTDC) were reduced by 33.33%, 32.37%, and 11.21%, respectively, compared with those of diesel fuel. The fuel blend B20 + 30% BHA (25 bTDC) showed the highest brake thermal efficiency of 14.52% at peak load condition. A multi-output regression deep long short-term memory (MDLSTM) model was designed to predict the performance and emissions of CI engines operating with varied fuel mixtures. The average RMSE and  $R^2$  values for the proposed MDLSTM were 0.38 and 0.9579, respectively.

**Keywords:** machine learning; injection timing; BHA; MDLSTM; RSME; antioxidants



**Citation:** Venkatesan, E.P.; Murugesan, P.; Narayana Pichika, S.V.V.S.; Janaki, D.V.; Javed, Y.; Mahmoud, Z.; Saleel, C.A. Effects of Injection Timing and Antioxidant on NO<sub>x</sub> Reduction of CI Engine Fueled with Algae Biodiesel Blend Using Machine Learning Techniques. *Sustainability* **2023**, *15*, 603. <https://doi.org/10.3390/su15010603>

Academic Editor: Antonio Galvagno

Received: 7 October 2022

Revised: 21 December 2022

Accepted: 26 December 2022

Published: 29 December 2022



**Copyright:** © 2022 by the authors. Licensee MDPI, Basel, Switzerland. This article is an open access article distributed under the terms and conditions of the Creative Commons Attribution (CC BY) license (<https://creativecommons.org/licenses/by/4.0/>).

## 1. Introduction

Increasing energy consumption and pollution make research on renewable energy sources increasingly crucial [1]. The usage of fossil fuel in internal combustion engines leads to a number of environmental problems [2]. A fuel called biodiesel is created using catalysts

and vegetable oils. The majority of developing nations experience environmental pollution due to fossil fuel usage, and biodiesel provides a solution to this issue [3]. Researchers selected biodiesel after taking into account its economic, environmental, and sustainable characteristics [4]. In order to make biodiesel commercially viable, it is essential to weigh the benefits of using a low-cost, nonedible oil to reduce production costs [5].

“The use of vegetable oil for engine fuel may appear minor today but such oil may become, in the course of time, as vital as petroleum”, wrote Rudolf Diesel regarding his engine that ran on peanut oil [6]. Fossil fuels are mostly found in a few locations worldwide, as is generally known. Many researchers have worked diligently to use vegetable oils as a motor fuel as they cut down on pollution and the demand for fossil fuels. Vegetable oils are renewable and emit no emissions; therefore, they are the most significant and have the most potential as fossil fuel substitutes [7].

They have a poor heat capacity and high viscosity, which leads to gum formation, thermal oxidization, and reduced engine endurance. Engines may run poorly and sustain harm if these oils are used without any changes. Contamination develops and sticks to piston rings due to the direct use of vegetable oil. Therefore, some preparation work is needed before using vegetable oils as fuel. Vegetable oils can be made useable by using a variety of techniques. The most well-liked of these is transesterification. There are two methods to extract algae oil: one is solvent extraction, and the other one is the transesterification process. The solvent extraction method uses the alcohol *n*-hexane as the solvent and was used to obtain algae oil. Using this method, dry algae biomass was converted to 28% of the algae oil. Algae biodiesel was produced by adding methanol and potassium hydroxide to the transesterification process. The optimum results obtained with 20% biodiesel were then compared with all other tested fuels. Then, the increased brake thermal efficiency (BTE) and the brake-specific energy consumption (BSEC) from the B20 blend were compared with mineral diesel fuels. B20 was also compared with mineral diesel fuel based on its ability to gradually reduce nitrogen oxides and smoke characteristics in a diesel engine (the B50 biodiesel blend is similar to and interchangeable with the B20 mix) [8–11]. If biodiesel from different strains is used, some pollutants can be reduced, but an increase in nitrogen oxides is frequently seen, which is linked to greater combustion chamber temperatures. Emulsions offer a viable option with considerable reductions in CO<sub>2</sub> and NO<sub>x</sub> when used in place of blends or straight biodiesel. The blends designated as B20, B30, B40, and B100 were used in the studies, which involved biodiesel in five ratios. Compared to diesel fuel, the tested blend B20's brake-specific fuel consumption (BSFC) at full load was nearly identical to that of the basic diesel fuel's BTE, and vice versa [12–22].

Compared with diesel fuels, the B20 blend had somewhat lower emissions characteristics for smoke, nitrogen oxides, and hydrocarbons [23]. To lessen the fuel's density and viscosity, biodiesel was extracted using the traditional transesterification procedure. Kar-bia seed was used to create a B20 fuel blend, which was then tested in a traditional engine. Compared with diesel fuels, B20's performance attributes improved. The B20 blend fuel's emissions characteristics, specifically its carbon monoxide and particle emissions, could be reduced, with the exception of nitrogen oxide pollution. Finally, it can be said that B20 fuel, which is made from used cooking oil, has the potential to lessen environmental pollution [24].

Numerous studies are now concentrating on biodiesel with antioxidant compounds to improve performance and emissions characteristics. The *n*-octanol additive agents can be blended with fossil fuel and then contrasted with mineral diesel fuel. When *n*-octanol fuel was added to biodiesel, the BTE went up, while the BSFC went down. When *n*-octanol was added to biodiesel, the emissions characteristics of nitrogen oxides, carbon monoxide, and hydrocarbons decreased. The results were then compared with those of base diesel fuel [25].

Waste plastic oil was recovered by applying the pyrolysis method, and then biodiesel and *n*-butanol were combined to drive a standard diesel engine. Waste plastic oil was mixed with *n*-butanol. The results were then compared with those of diesel fuel after the addition

of 10% n-butanol to the fuel to lower the oxides of nitrogen. Soot emissions dropped, whereas hydrocarbon emissions increased. When n-butanol was added, performance traits such as BTE improved. Then, they were compared with those of diesel fuel [26]. An increase in n-propanal caused the smoke opacity to decrease, and the use of PR10, PR20, and PR30 blend fuels caused the smoke opacity to decrease by 13.33%, 33.33%, and 60%, respectively. In contrast, as the exhaust gas recirculation (EGR) rates increased, the smoke opacity also increased.

The results of these three blends were compared with those of pure diesel fuel as they demonstrated that the oxides of nitrogen increased without EGR and dropped when EGR rates increased. Finally, it was determined that, compared with plain diesel, adding n-propanal to fuel might lower CO, HC, and NO<sub>x</sub> emissions [27]. The three concentration volumes with percentages of 10%, 20%, 30%, and 45% were used to test the n-pentanol/diesel fuel blends. According to the test results, using 45% n-pentanol/diesel in a conventional diesel engine significantly reduced smoke and nitrogen oxide emissions. When EGR rates increased, nitrogen oxides reduced relative to clean diesel, whereas smoke emissions increased by 20%.

Parameters of diesel engines, such as injection timing and injection pressure, are another area of interest for researchers. Modifications to the piston, such as heat barrier coating and piston design characteristics, have been the subject of research. The current study focuses on the diesel engine's injection time to lower nitrogen oxide emissions. Dual biofuel (rubber seed and jatropha) was used in a single-cylinder diesel engine by delaying the injection timing from the standard 24° to 21°. The percentages of biodiesel added to regular fossil diesel were 20% (B20), 40% (B40), and 60% (B60). The effect of various injection times on the diesel engines was determined in this study using a dual biofuels system.

Brake-specific fuel consumption, CO (carbon monoxide), NO<sub>x</sub> (nitrogen oxides), and UHC were the performance and emissions characteristics taken into consideration for the tests (unburned hydrocarbon). The results showed that the SFC content of the B20 blend was lower than that of pure diesel fuel, whereas the SFC content of the B40 and B60 blends was greater than the B20 blend. In addition, it was found that the emissions of CO and UHC reduced, but those of NO<sub>x</sub> increased as the biodiesel content of the fuel mixture increased. The authors conducted their research with a variety of different fuels, including mineral diesel, alcohol, and biodiesel.

Increased thermal efficiency, increased fuel efficiency, reduced CO emissions, and increased NO<sub>x</sub> emissions were all reported when diesel fuel injection timing was optimized. Reduced cylinder pressure, low peak temperature, and delayed injection timing all contributed to decreased NO<sub>x</sub> emissions. As fuel injection was delayed, both combustion time and cylinder peak pressure diminished, which resulted in lower fuel efficiency and higher fuel consumption. However, enhanced combustion, greater fuel efficiency, the fuel's capacity for oxidation, and increased cylinder temperatures led to a decrease in O<sub>2</sub>, carbon, and UBHC emissions.

Diesel–biodiesel fuel blends often resulted in greater CO and HC emissions; however, the NO<sub>x</sub> emissions reduced when the timing of the injection was delayed. To investigate combustion and performance parameters, evaluated biodiesel–diesel–ethanol blends in CI engines with altered injection times. The fuel blends were tested in this experiment using a Euro III multi-cylinder diesel engine. The test engine's fuel consumption rate then decreased by 4% with modified injection timing, and a 20% reduction in fuel consumption was noted for high torque conditions. Beginning with a ratifying specific fuel consumption trend, the ethanol blend increased up to 30% for injection time adjustment. When tested with CI and spark-ignition (SI) engines, the ethanol produced specific energetic fuel consumptions between 7.1 and 12.6 MJ/kWh for the CI engine and a spectrum range between 10.7 and 13.5 MJ/kWh for the SI engine. The engine's injection timing changed due to the presence of ethanol, and the optimized timing predicted the correct trend. The 1° advance

in timing resulted in a 5% increase in the amount of ethanol that was present in the test fuel mixes.

Predicting engine performance and emissions using advanced artificial intelligence serves as a useful tool to reduce the number of experiments and simulations analyzed. Ref. [28] investigated the effect of an orange peel biofuel blend augmented with graphene oxide nanoparticles on the performance characteristics of a CI engine. BTE, BSEC, and emissions for different fuel blends were evaluated using an experimental approach. Finally, an artificial neural network (ANN) prediction model was developed which used the experimental data to predict the BTE, BSEC, and emissions of different fuel blends. The developed ANN model showed a good prediction accuracy with the mean absolute percentage error ranging from 0.84 to 4.12. Ref. [16] investigated the emissions performance of a micro gas turbine that operated with different blends of jet fuel with microalgae blends (20% and 30%). In total, 51 fuel combinations were experimentally evaluated to find the performance and emissions characteristics. A decrease in CO, CO<sub>2</sub>, and NO<sub>x</sub> emissions was observed for certain fuel blends. A long short-term memory (LSTM) network was developed using the experimental data to predict the performance and emissions characteristics of the micro gas turbine for different fuel blends.

The literature review demonstrated that biodiesel's performance was enhanced and harmful pollutants were reduced owing to the use of various additives. Normally, in a diesel engine, the oxides of nitrogen, HC, and CO are high when using injection timing techniques. To overcome this problem, some additives, such as *p*-phenylenediamine (PPDA), A-tocopheryl acetate, L-ascorbic acid, and butylated hydroxyanisole (BHA), can be added. Many studies have been done using *p*-phenylenediamine (PPDA), A-tocopheryl acetate, and L-ascorbic acid, but only a few studies have been done using BHA. The novelty of this work includes increasing the performance of the engine to cut down the pollution coming out from the exhaust. Algae biodiesel played a very important role in this investigation. The percentage of antioxidants was increased to get optimum results. Many studies already considered the addition of 30% antioxidants with biodiesel to achieve optimum results. The diesel engine's performance and emissions characteristics were improved by adjusting the injection timing and adding fuel additives. The current study used different injection timings, such as 21°, 23°, and 25 °bTDC, algal biodiesel, as well as some antioxidant compounds in the diesel engine. The outcomes were compared with those of diesel fuel. Furthermore, a multi-output regression deep LSTM (MDLSTM) model was developed to predict the CI engine performance and emissions characteristics of different fuel additive ratios.

In Tables 1 and 2, two symbols are used, including an upward symbol and a downward symbol. The upward symbol represents an increase, and the downward symbol represents a decrease.

**Table 1.** Previous studies showing the performance and emissions characteristics using biodiesel and injection timing.

No.	Fuel	BTE	BSFC	CO	NO <sub>x</sub>	HC	Smoke Opacity	Ref.
1.	Waste oil methyl ester (24 °bTDC)	↑	↑	↓	↓	↓	↓	[29]
2.	Algae oil methyl ester (25 °bTDC)	↑	↓	↓	↑	↓	↓	[30]
3.	Karanja oil (24 °bTDC)	↑		↓	↑	↓	↓	[31]
4.	Mahua oil (25 °bTDC)	↑	↑	↓	↓	↓	↓	[32]
5.	Roselle biodiesel oil (19–25 °bTDC)	↓	↓	↓	↑	↓	↓	[33]

**Table 2.** Properties of fuels.

Properties	Diesel	Algae Biodiesel (B20)
Density (kg/m <sup>3</sup> ) at 15 °C	830	836.5
Viscosity (mm <sup>2</sup> /s) at 40 °C	2.9	3.26
Cetane Number	45–55	48.88
Calorific Value (MJ/kg)	42.5	42.2
Flash Point (°C)	76	86.6
C (%)	87	84.9
H (%)	12.5	12.45
O (%)	0.4	2.48

## 2. Outline of Algae Biodiesel

Improving the biomass per acre of algae is essential to use it as a renewable fuel. According to some researchers, algae may be 10–100 times more productive than bioenergy feedstock. Realizing the potential of sustainable and affordable algal biofuels demands high production in the real world. Algae may be transformed into fuels for automobiles, trains, planes, and trucks. Carbohydrates, proteins, and lipids or natural oils are the three primary components that make up the biomass of algae. The majority of natural oil produced by microalgae is in the form of triacylglycerol, which is an appropriate kind of oil to use when manufacturing biodiesel; therefore, microalgae are the exclusive focus of attention for preparing biodiesel in the field of algae. In addition to biodiesel, microalgae have potential to produce a variety of other forms of usable energy. Certain types of algae are capable of producing hydrogen gas, given the right cultivation circumstances. In addition, biomass from algae can be burned like wood, or it can be digested anaerobically to produce methane, which can then be used to generate heat and electricity. Pyrolysis is another method that can be used to process algal biomass to produce crude bio-oil.

### 2.1. Production of Algae Biodiesel

A number of algae generation methods are currently being worked on, including open lakes, closed photo-bioreactors, maturation tanks, half-breed frameworks, and other techniques that combine these different techniques. Basically, there is no single approach to develop algae on a large scale, and this adaptability is one of algae's best qualities.

Most of the time, the methodology chosen is structured exclusively to boost algae growth and development to then create fuel, synthetic substances, or other modern items. How precisely these frameworks work depends on where they are found and the ideal end result. This study investigates a few imaginative green growth development frameworks that are currently being studied in the United States. Figure 1 shows the production of algae biodiesel.

### 2.2. Prepared Fuels

The world's fastest-growing species are algae. Open ponds, photobioreactors, and closed systems are industrial reactors for algae culture. Algae are a crucial source of biomass. One day, algae will be a competitive source of biofuel. Algae can serve as a more efficient and disadvantage-free alternative to oil-based fuels. Algae are among the plants with the highest rate of growth, and nearly half of their weight is oil. Biodiesel is derived from algae plants with help from the transesterification process. The density and viscosity of biodiesel are very close to those of diesel fuel. The prepared biodiesel blend B20 (which uses 20% biodiesel + 80% diesel) is added along with the antioxidant agents. The antioxidant agents are added to the biodiesel in different proportions of butylated hydroxyanisole, such as 30 ppm. The fuel blend prepared includes B20 (20% biodiesel + 80% diesel + 30 ppm BHA) to find the effect of injection timing on the performance, combustion, and emissions

characteristics of diesel engines operated under a full-load condition. These results were compared with mineral diesel fuels. Table 2 shows the properties of the prepared fuel.

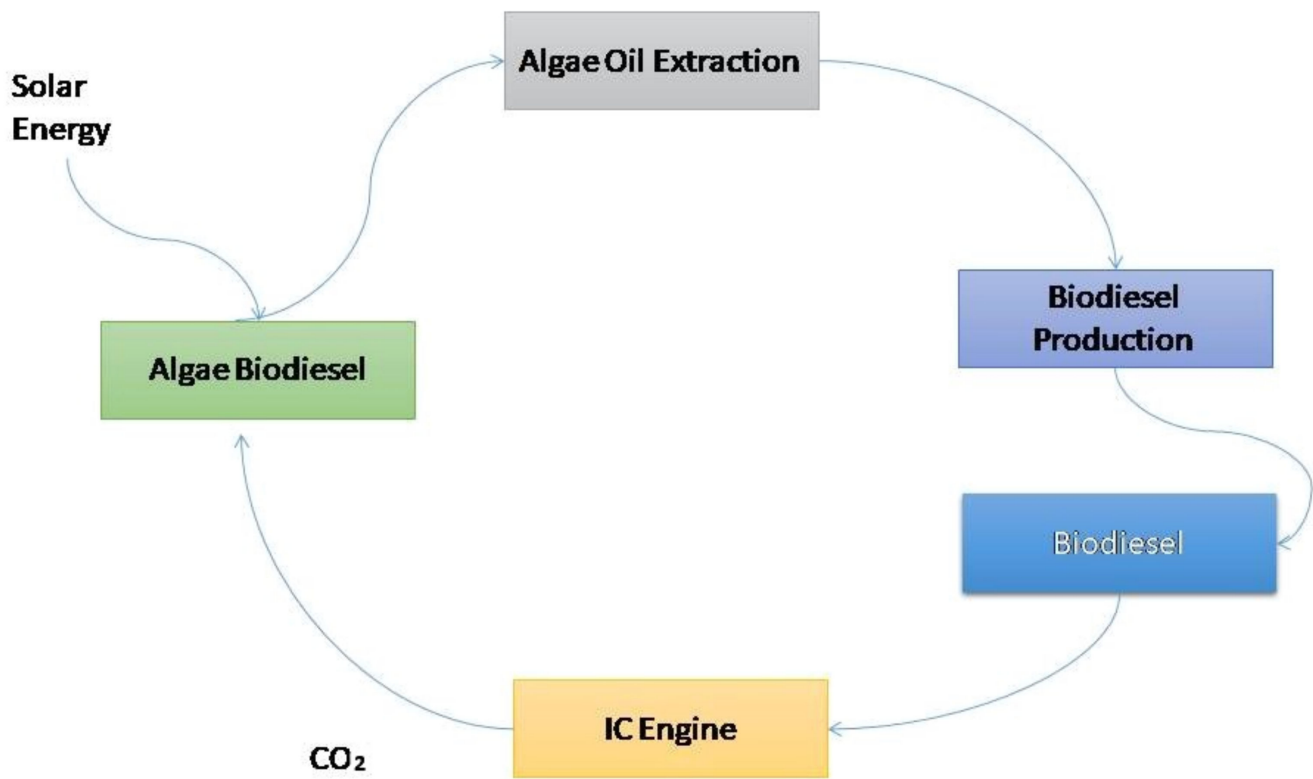


**Figure 1.** Production of algae biodiesel.

### 2.3. Injection Timing Adjustments

Typically, injection time is changed to increase engine power. Power can be increased by moving the injection time forward. Timing may occasionally be changed to the reverse direction to address smoke or latency issues. Advancing an engine's timing moves combustion forward in time (i.e., modifying the timing makes ignition happen sooner). The reverse of advancing an engine's timing is retarding it. It occurs when timing is adjusted so that ignition happens later than the manufacturer's original recommended time. Depending on the type and year of the engine, a person can change injection timing in a number of ways. The ECM must be programmed, the fuel injection pump must be adjusted, the camshaft must be replaced, and the cam followers or gaskets must be replaced.

### 2.4. Engine Setup

Figure 2 shows an experimental single-cylinder, air-cooled, vertical, direct-injection diesel engine. It generates 4.4 kW at 1500 rpm and is linked to an eddy current dynamometer. An anti-pulsating drum, an air heater, and air temperature measuring equipment are on the engine's inlet components. An EGT indicator, an exhaust gas analyzer, and a smoke sampler are engine exhaust components. A separate fuel-measuring device assesses algae biodiesel blend usage. The test setup includes a 64-bit DAQ system to measure crank angle and cylinder pressure [34–37]. The data systems are used to find the combustion parameters. An AVL exhaust analyzer was used to determine the smoke opacity. Uncertainty was calculated in this study.

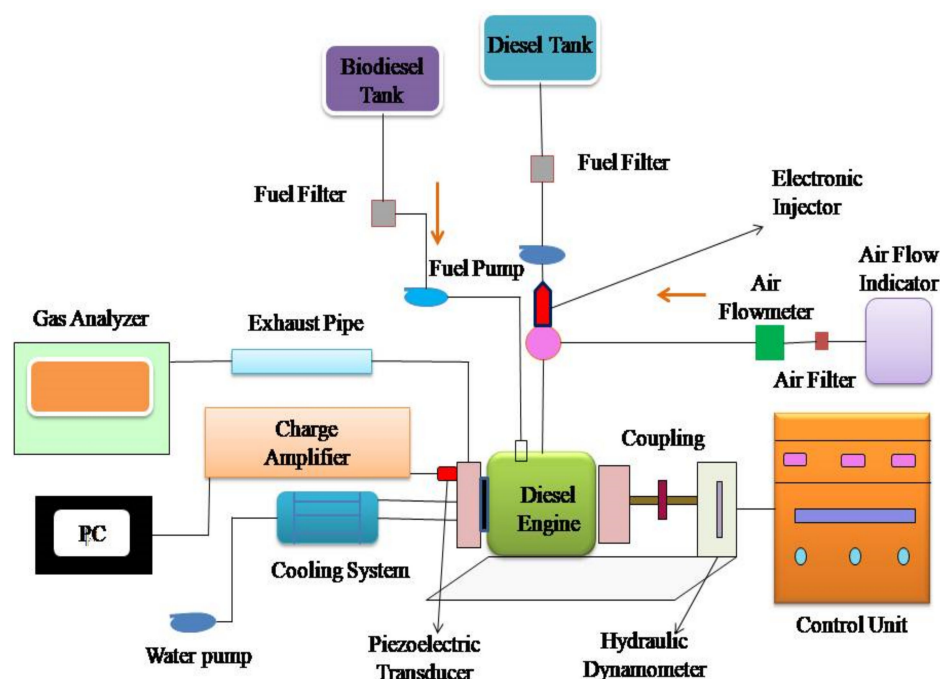


Figure 2. Engine setup.

### 3. Result and Discussion

#### 3.1. Oxides of Nitrogen

The variation in oxides of nitrogen and all the tested fuels related to brake load under a full-load condition are shown in Figure 3. In general, the diesel engine produces lower oxides of nitrogen at starting load condition, and they increase under full-load condition. After adding the BHA antioxidants to the fuel, the oxides of nitrogen increase gradually compared with the neat diesel fuel because of increased oxygen content in the fuel [38]. The fuel blend B20 + 30% BHA (23 °bTDC) shows reduced oxides of nitrogen by 43% compared with the conventional fuel (D100) under peak load condition. This is the result of the cooling impact generated by high latent vaporization heat of BHA and greater oxygen content which produce a low peak temperature during the combustion process. B20 + 30% BHA (21 °bTDC) had 49% less oxides of nitrogen than diesel fuel as a result of the antioxidants' ability to inhibit the formation of peroxy-free radicals by reacting with aromatic amines. The fuel blend B20 + 30% BHA (25 °bTDC) had 9.9% greater NO<sub>x</sub> emissions compared with diesel fuels, which may be attributed to the creation of peroxy-free radical forms and an increase in the combustion temperature. An unpaired electron in a molecule, known as a free radical, determines the rate of oxidation for that molecule.

#### 3.2. Smoke

The variation in smoke opacity and all the tested fuels related to brake load at full-load condition is shown in Figure 4. Smoke opacity emissions are high in the neat biodiesel compared with all the tested fuels. In previous studies, algae biodiesel showed a high smoke opacity [6,26]. Smoke opacity decreases when BHA antioxidants are combined with algae biodiesel and diesel fuel due to an increase in fuel oxygen in the blends and oxygen concentration, even in fuel-rich regions. At 23 °bTDC, diesel fuel shows less smoke opacity than B20 + 10% BHA–21 °bTDC fuel with standard injection timing. That could be due to the greater cetane number of diesel and the delay period resulting from the different injection timings of 23° and 21 °bTDC. At maximum engine loads, the 25 °bTDC fuel shows reduced smoke emissions compared with other fuels. The reason for minimal emissions is that the engine operated with the maximum extent of injection timing of 25 °bTDC, which increases the residence time for fuel and air mixing and results in clean,

regulated combustion [39–43]. These combined actions finally reduce the smoke emitted by the advanced injection timing.

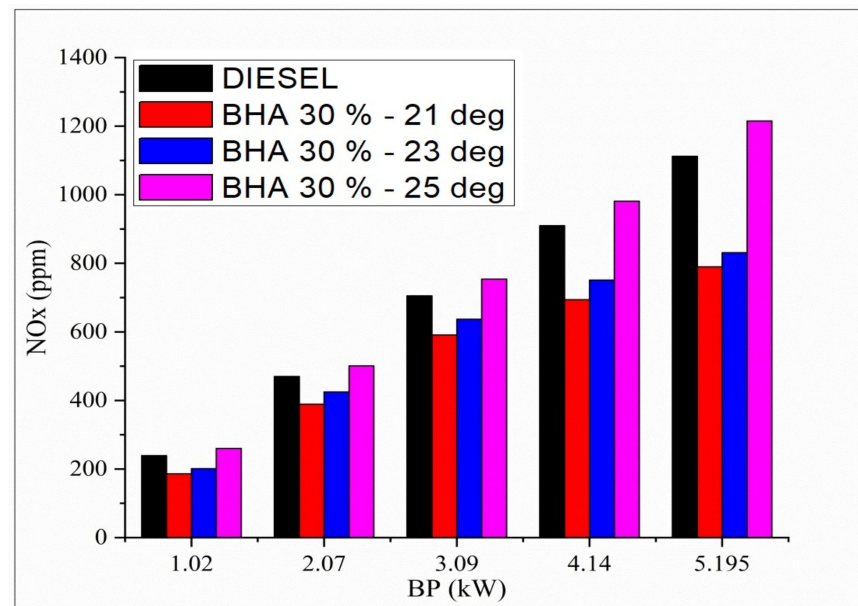


Figure 3. Variations in brake power and oxides of nitrogen in all fuel blends.

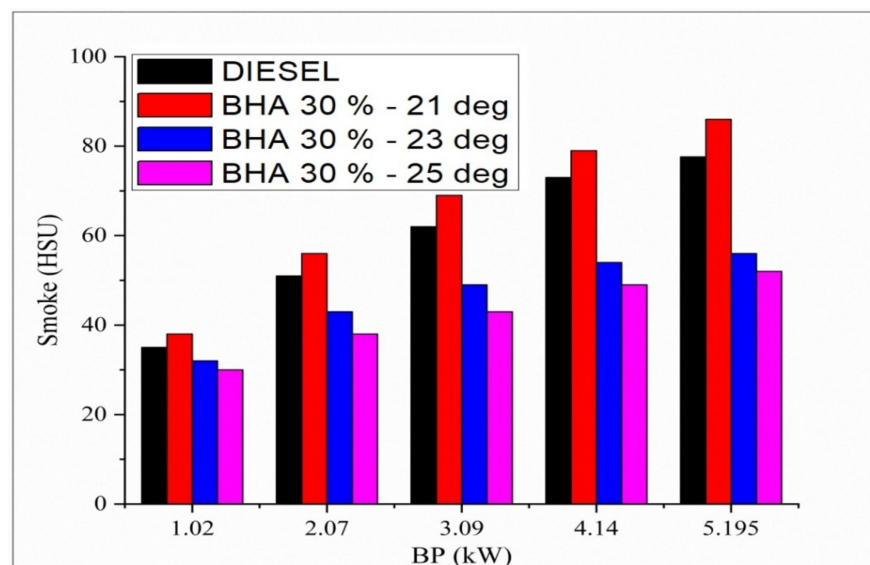


Figure 4. Variations in brake power and smoke in all fuel blends.

### 3.3. Carbon Monoxide

Figure 5 shows the variation of carbon monoxide and all the tested fuels related to brake load at full-load condition. Carbon monoxide is formed in the diesel engine because of incomplete combustion caused by the unavailability of oxygen content. Carbon monoxide emissions increase during engine start; however, the addition of BHA antioxidants to the fuel reduces carbon monoxide emissions in diesel engines. Owing to its short burning time and lack of preparation time in the combustion bowl, the blend B20 + 30% BHA (21 °bTDC) produces the highest carbon monoxide levels (0.21%) of all the tested fuels. The addition of BHA antioxidants and high temperatures under high-load conditions cause the blend B20 + 30% BHA (25 °bTDC) to show low emissions of 0.16% compared with diesel fuel [44–48]. A longer delay period enhances the spray pattern and atomization of fuel, which then enhances combustion in the cylinder.



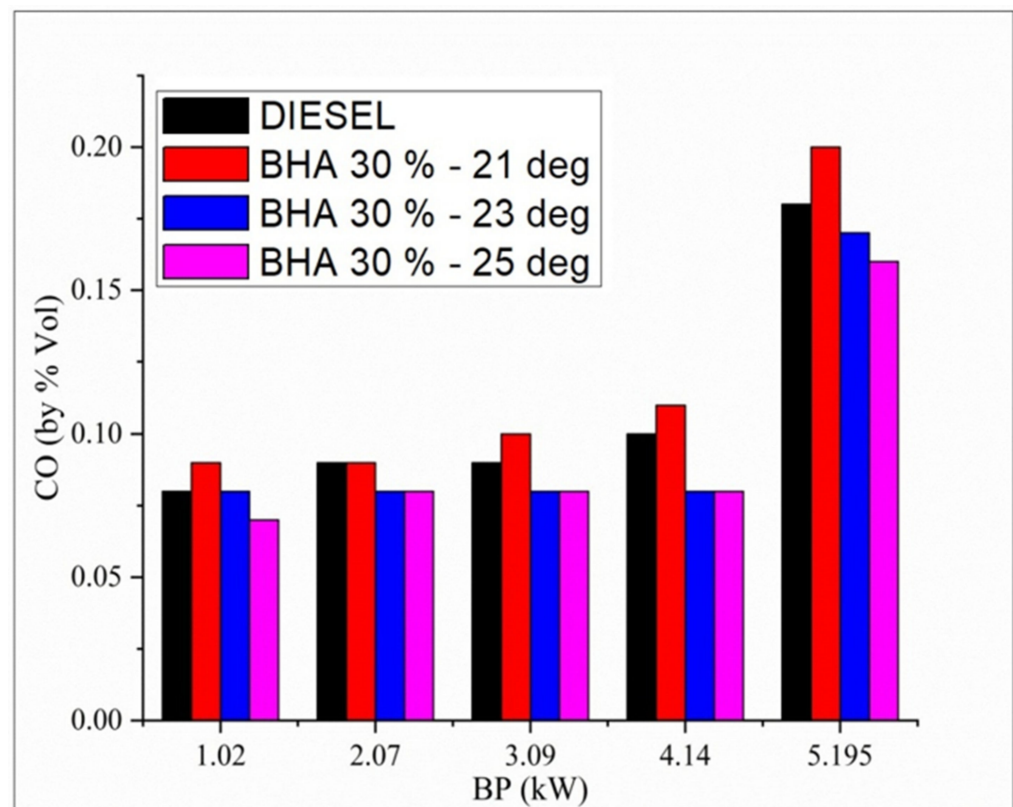


Figure 5. Variations in brake power and carbon monoxide for all fuel blends.

### 3.4. Hydrocarbon

Fluctuations in carbon monoxide and all tested fuels in relation to brake load under full-load condition are shown in Figure 6. The presence of unsaturated hydrocarbons that are strengthened during combustion enables neat biodiesel to generally have higher hydrocarbon emissions compared with diesel fuel. The atomization rate is low when using a blend of B20 and 30% BHA (21 °bTDC) due to partial combustion and a shorter delay period. Standard diesel at peak load and normal timing records low HC emission. The blend B20 + 30% BHA (25 °bTDC) provides low hydrocarbon emission compared with normal diesel fuel [49–52]. Improved injection timing and a longer ignition delay and improve evaporation and precombustion preparation of the air–fuel mixture, which results in enhanced combustion.

### 3.5. Performance Characteristics (Brake Thermal Efficiency)

Deviations in BTE regarding brake power for the conflation impact of different injection timings with B20 + 30% BHA fuel are shown in Figure 7. Raw algal biodiesel has a low thermal efficiency compared with all other evaluated fuels due to the additional energy required to break down the significant hydrocarbon chains and the main aromatic compounds that comprise 40% of the algae. The BTE of B20 + 30% BHA (21° BTDC) is low in this test compared with all the fuels and all injection timings. It is connected with the retardation of fuel injection timing at 21 °bTDC in the engine. Fuel injection retardation has insufficient time for air–fuel mixing, and poor combustion is noted. In contrast, advancing the fuel injection timing at 23° and 25 °bTDC results in an improved combustion process, and hence, a higher BTE is observed [53,54]. This is due to enough residence time for air–fuel mixture preparation in the cylinder with a longer combustion duration.

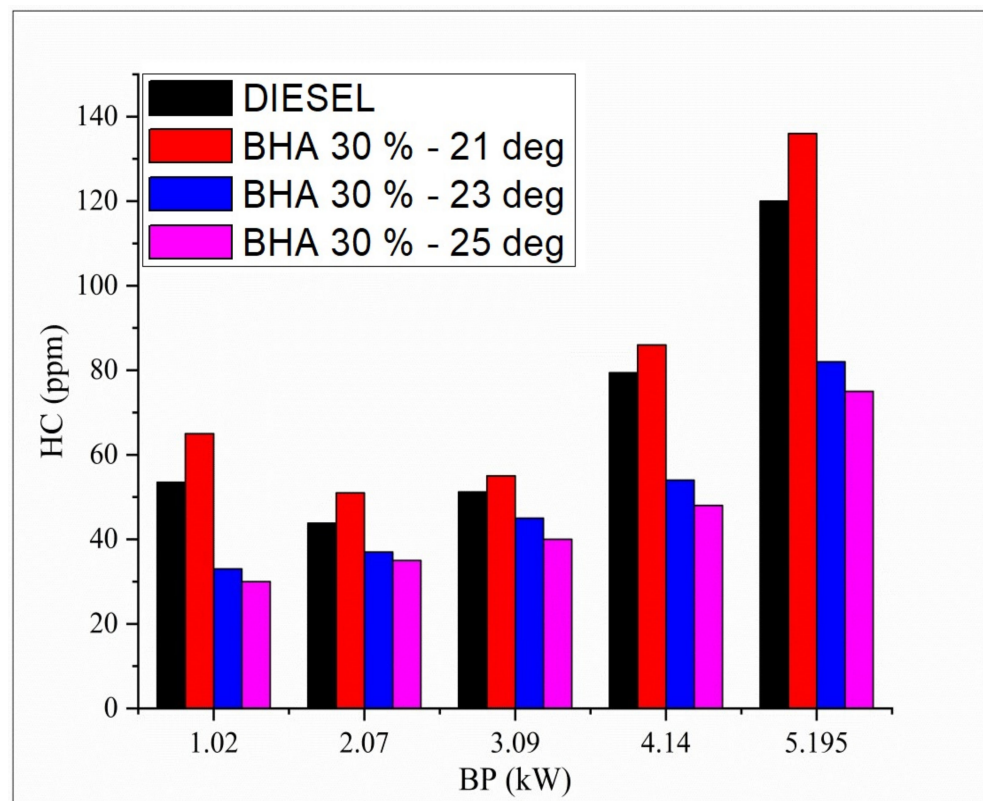


Figure 6. Variations in brake power and hydrocarbon in all fuel blends.

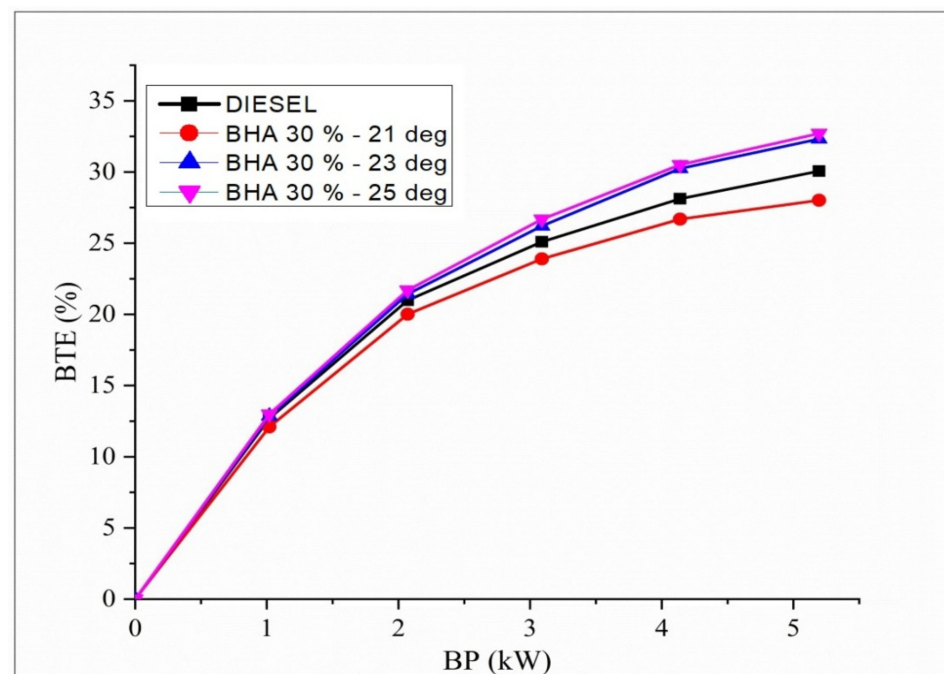
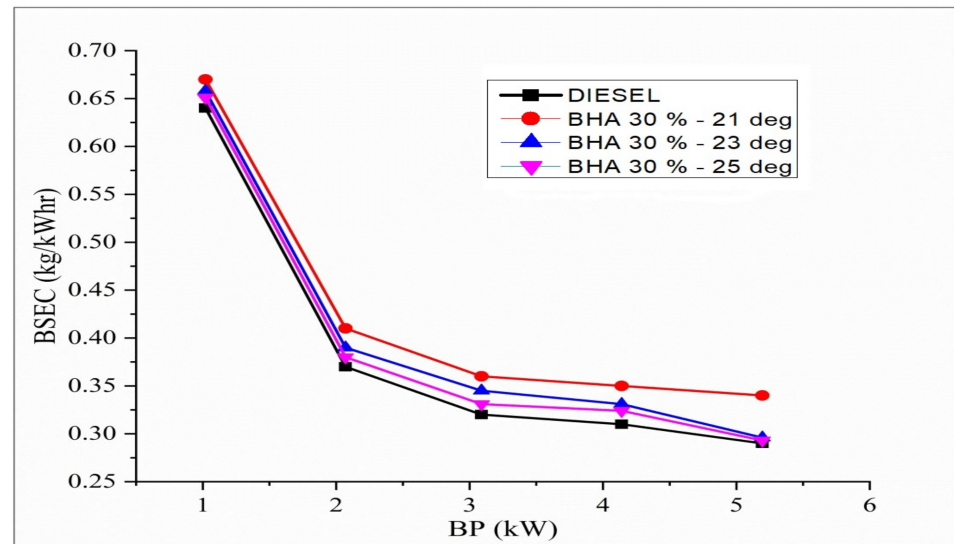


Figure 7. Variations in brake power and BTE in all fuel blends.

### 3.6. Brake-Specific Energy Consumption

The trend for BSFC variation in brake power for different injection timings and with B20 + 30% BHA (21 °bTDC) fuels is shown in Figure 8. The calorific content exerts an important effect on fuel consumption. At a regular injection timing of 23 °bTDC, the BSEC of standard diesel fuel is comparable to that of all other fuels. B20 + 30% BHA (21 °bTDC) has greater BSEC than diesel due to retarded fuel injection pressure at 21 °bTDC. While

the retardation process has a higher combustion temperature and pressure, it does not have sufficient time for complete burning. Hence, a more significant amount of fuel is consumed during the retardation process. B20 + 30% BHA (25 °bTDC) has lesser BSEC compared with B20 + 30% BHA (21 °bTDC) and B20 + 30% BHA (23 °bTDC). This result is due to the practical usage of fuel by keeping the burning process very close to TDC, which improves evaporation in the bowl. Hence, a lower BSEC is observed for the biodiesel blend at peak load.



**Figure 8.** Variations in brake power and BSEC in all fuel blends.

### 3.7. Combustion Characteristics Cylinder Pressure

Figure 9 shows the differences between cylinder pressures dependent on crank angle for B20 + 30% BHA fuels combined with diesel fuel. B20 + 30% BHA (21 °bTDC) shows low peaks of combustion pressure compared with all the other fuels. The low cylinder pressure results from poor atomization and a shorter preparation time at lower injection timing extents. At B20 + 30% BHA (25 °bTDC), the fuel gives inflated cylinder pressure on par with all the injection timings and fuels. Owing to the injection timing of 25°, the air–fuel mixture, evaporation rate, and ignition delay period are improved. Compared with B20 + 30% BHA at 21°, diesel fuel at 23 °bTDC has a negligible effect on cylinder pressure. Variations in time and properties, such as heating value and cetane number, lead to an increase in pressure. B20 + 30% BHA (25 °bTDC) may be recommended for B20 + 30% BHA-powered diesel engines.

### 3.8. Heat Release Rate

Figure 10 illustrates the differences between the heat release rate (HRR) and the crank angle for B20 + 30%BHA diesel fuels accompanied by B20 + 30% BHA (23° bTDC), B20 + 30% BHA (21 °bTDC), and B20 + 30% BHA (23 °bTDC). The HRR graph indicates that B20 + 30% BHA (21 °bTDC) has a lower magnitude compared with all the other fuels. This finding may be due to the presence of antioxidants in the fuel and a lower extent of injection timing of 21 °bTDC, which results in depressed combustion. The B20 + 30% BHA (25 °bTDC) timing has maximum HRR in the cycle when it is equated with all other injection timings. This result is likely due to an increase in the delay period and the influence of HRR on the premixed burning phase and on the mixed-controlled burning phase, which results in an increase in HRR.

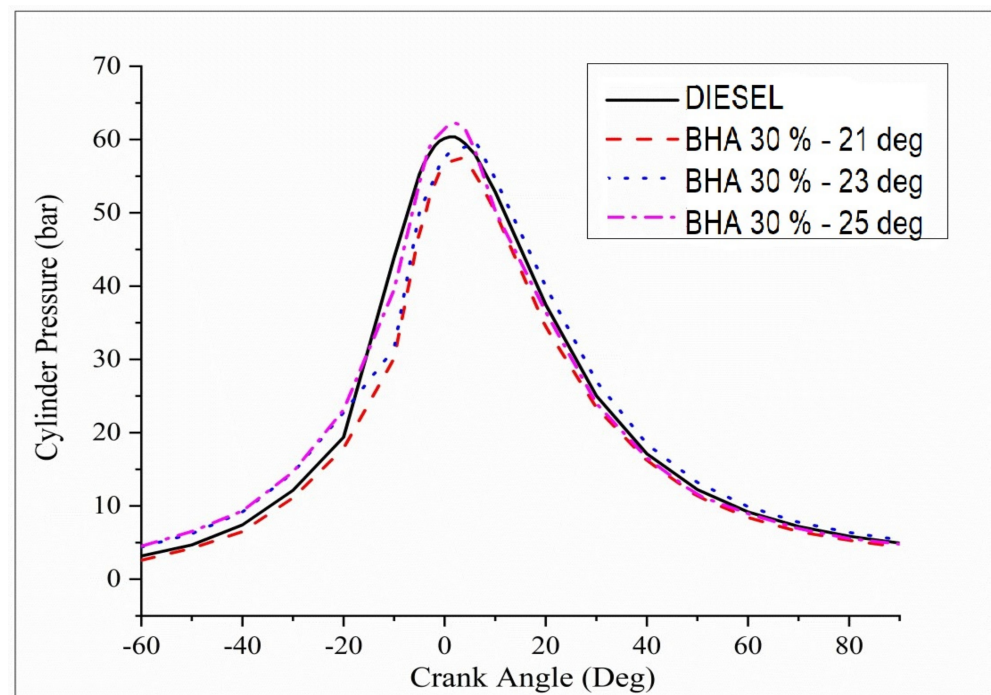


Figure 9. Variations in brake power and cylinder pressure in all fuel blends.

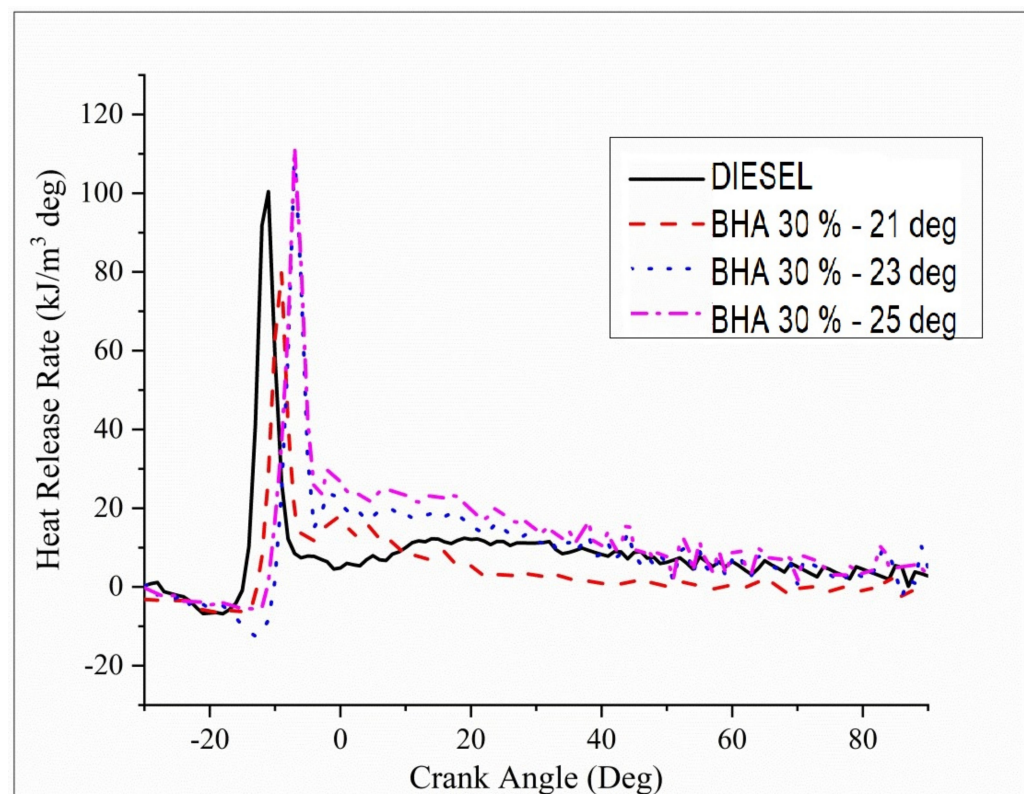


Figure 10. Variations in brake power and heat release rate for all fuel blends.

#### 4. LSTM Prediction Model

In this work, an MDLSTM model was developed to predict the CI engine performance and emissions for different fuel blends due to its ability to find nonlinear relations in data. The LSTM, which is a recurrent neural network (RNN), was invented by, and it can learn long-term dependencies within data [55]. Brake power (BP) and fuel blends with

different pressure angles were taken as input for the MDLSTM model. The MDLSTM model was developed in Python with Keras and Scikit learn libraries [56,57] with three inputs, including fuel blend, injection pressure, and brake power. For given combinations of the input, six outputs, namely BTE, BSEC, CO, HC, NO<sub>x</sub>, and smoke, were the predicted outcomes. The MLSTM model was trained using the experimental results. The dataset consisted of three inputs and six outputs and had dimensions of  $25 \times 6$ . This dataset was split into training (80%) and testing (20%) datasets. The root mean square error (RMSE) was taken as the performance indicator of the prediction for the MDLSTM. The lower the RMSE, the better the prediction. The MDLSTM consisted of four stacked LSTM layers, and each layer had 150 neurons trained with 21 samples. A batch size of two was taken with the hyperparameter of 200 epochs. The RMSE values obtained for BTE, BSEC, CO, HC, NO<sub>x</sub>, and smoke were 0.443, 0.151, 0.045, 0.535, 0.512, and 0.61, respectively. Table 3 shows the observed and predicted values.

**Table 3.** The observed and predicted values.

	Experimental	Predicted
BTE (%)	28.43	28.54
	23.89	23.67
	26.12	25.2
	14.25	14.41
	24.12	24.34
BSEC (MJ/kW·h)	0.32	0.59
	0.37	0.48
	0.34	0.41
	0.65	0.51
	0.36	0.43
CO (% vol.)	0.17	0.25
	0.063	0.054
	0.14	0.084
	0.075	0.055
	0.07	0.065
HC (ppm)	126	125.7
	62	63.05
	88	87.7
	32	32.92
	40	40.5
NO <sub>x</sub> (ppm)	1150	1149.67
	244	243.97
	721	720.85
	201	200.58
	510	511
Smoke (%)	80	80.66
	15	14.15
	78	78.8
	32	32
	41	40.75

The authors made an MDLSTM model which predicted that the average RMSE would be under 0.38 and would be inside the proposed level. Additionally, the coefficient of determination ( $R^2$ ) was calculated to find the fitness of the MDLSTM regression model. The  $R^2$  values obtained for BTE, BSEC, CO, HC, NO<sub>x</sub>, and smoke are 0.9107, 0.9928, 0.8763, 0.9986, 0.9762, and 0.9928, respectively. Figure 11 shows overall combined graphs. The MDLSTM model has an average  $R^2$  value of 0.9579, which shows a good correlation between the predicted and experimental values. The correlation values for the experiments and the predicted values are shown in Figures 12–17. This examination similarly upholds the data expected for the test results. The created MDLSTM model is seemingly a productive instrument that can foresee the boundaries of the engine that are exceptionally close to the trial results and limit trial and error cost, time, and intricacy related to an exploratory review.

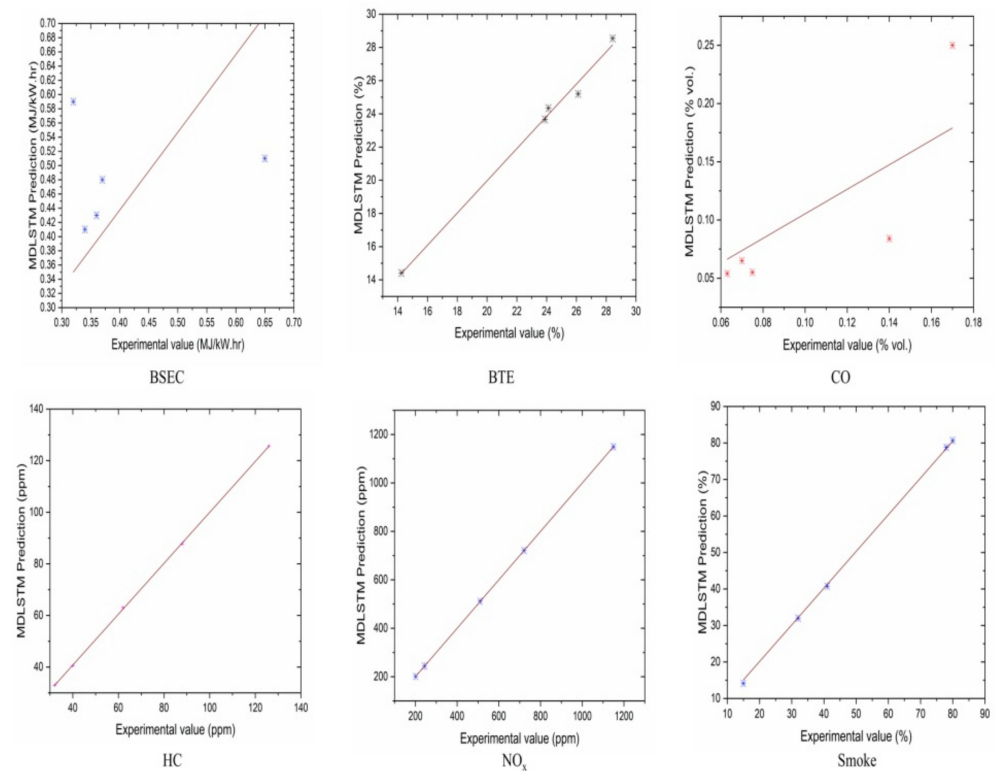


Figure 11. Combined results for all the graphs.

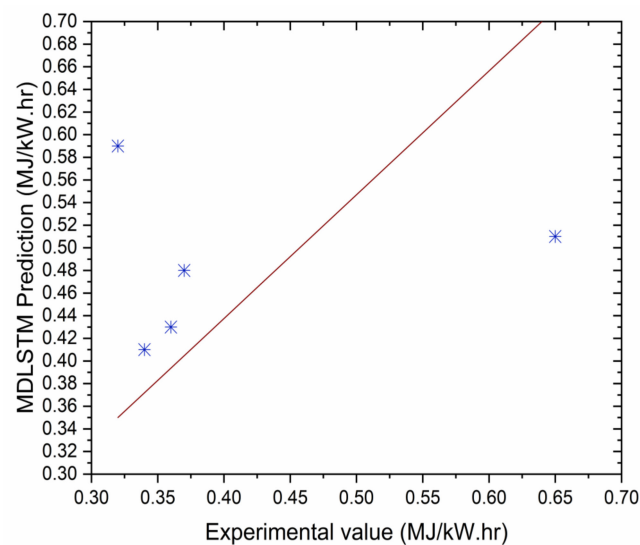


Figure 12. Correlation between MDLSTM predictions and experimental results for BSEC.

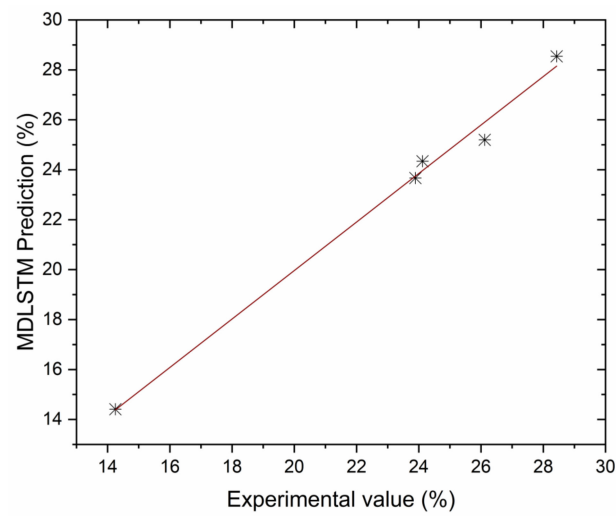


Figure 13. Correlation between MDLSTM predictions and experimental results for BTE.

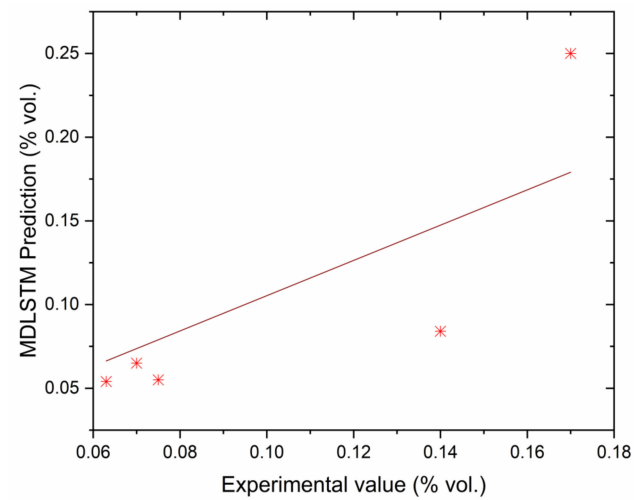


Figure 14. Correlation between MDLSTM predictions and experimental results for CO.

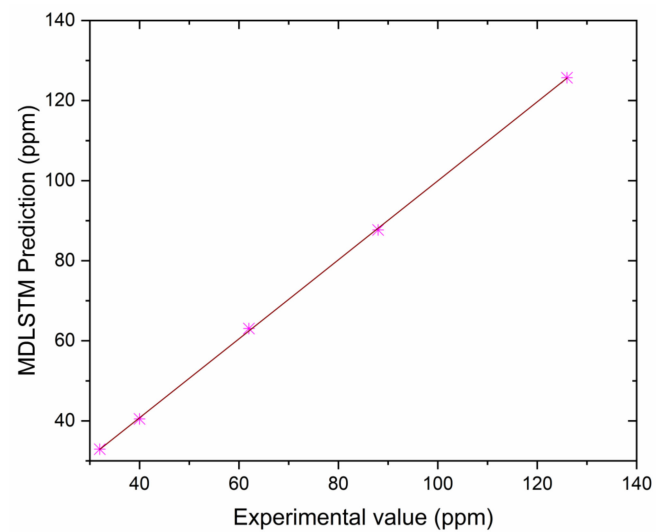
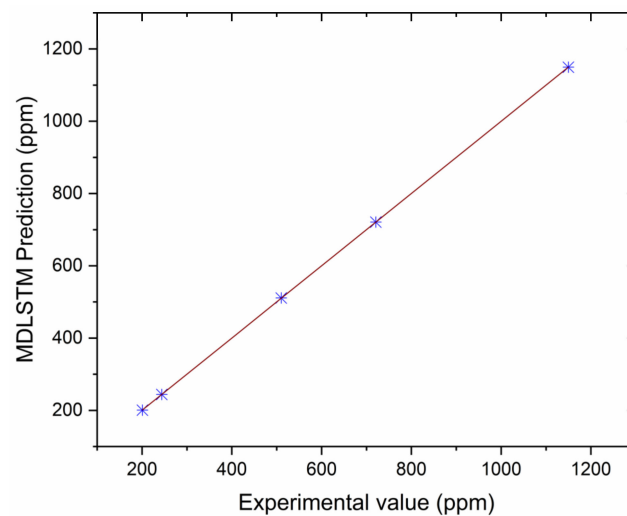
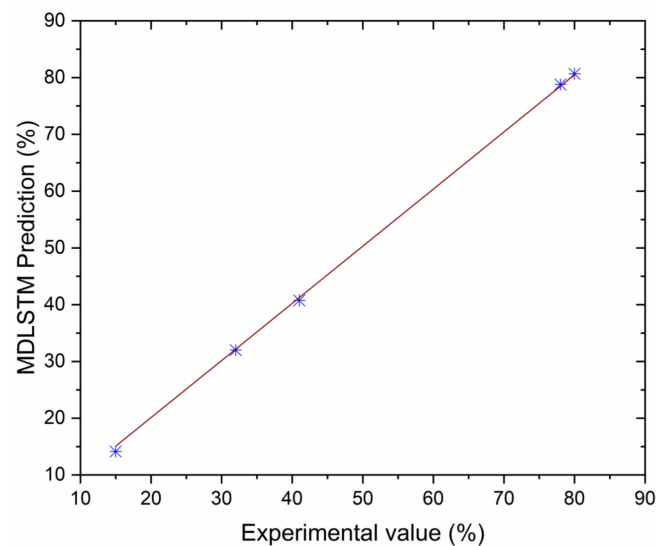


Figure 15. Correlation between MDLSTM predictions and experimental results for HC.



**Figure 16.** Correlation between MDLSTM predictions and experimental results for NOx.



**Figure 17.** Correlation between MDLSTM predictions and experimental results for smoke.

## 5. Conclusions

- Antioxidants suppress the formation of peroxy-free radicals by interacting with aromatic amines, which results in a 49% decrease in nitrogen oxides compared with diesel fuel.
- The engine is operated at its maximum injection timing of 25 °bTDC, which lengthens the time that fuel and air have to mix before combustion and provides a clean burn.
- The inclusion of BHA antioxidants due to high temperatures at a high load condition creates a low emission rate (0.16%) for the blend B20 + 30% BHA (25 °bTDC) compared with diesel fuels.
- Compared with regular diesel fuel, the blend B20 + 30% BHA (25 °bTDC) offers reduced hydrocarbon emissions. This finding might be ascribed to improved evaporation and a longer ignition delay, which improve preparation of the air–fuel mixture and result in a clean combustion.
- Improving the timing of fuel injection at 23° and 25° before top dead center leads to a more efficient combustion process, which results in a higher BTE. This is because the cylinder has a longer combustion duration and more time to settle and prepare the air–fuel mixture.
- Fuel at 25 °bTDC with B20 + 30% BHA increases cylinder pressure, which is comparable to all other fuels and injection timings. The enhanced air–fuel mixing, evaporation



rate, and ignition delay period created by a 25° injection timing are responsible for the higher performance.

- The proposed MDLSTM model can predict CI engine performances and emissions for various fuel blends with average RMSE and  $R^2$  values of less than 0.38 and 0.9579, respectively.

**Author Contributions:** Conceptualization, E.P.V.; formal analysis, P.M.; funding acquisition, D.V.J.; investigation, S.V.V.S.N.P.; methodology, E.P.V.; resources, S.V.V.S.N.P., C.A.S. and Y.J.; software, P.M.; supervision, Z.M.; visualization, S.V.V.S.N.P.; writing—original draft, Z.M., Y.J. and S.V.V.S.N.P.; writing—review and editing, S.V.V.S.N.P. All authors have read and agreed to the published version of the manuscript.

**Funding:** The authors are especially thankful to Prince Sultan University for paying the Article Processing Charges (APC) for this publication.

**Institutional Review Board Statement:** Not applicable.

**Informed Consent Statement:** Not applicable.

**Data Availability Statement:** Not applicable.

**Acknowledgments:** This research work was supported by the Research Center for Advanced Materials Science, King Khalid University, Ministry of Education, Kingdom of Saudi Arabia through grant number: RCAMS/KKU/015/22. Also, the authors would like to thank Prince Sultan University for supporting the research project.

**Conflicts of Interest:** The authors declare no conflict of interest.

## References

1. Resitoglu, I.A.; Keskin, A. Biodiesel production from free fatty acids and the effects of its blends with alcohol–diesel on engine characteristics. *Clean Technol. Environ. Policy* **2017**, *19*, 925–931. [[CrossRef](#)]
2. Varuvel, E.G.; Mrad, N.; Aloui, F.; Tazerout, M. Experimental analysis of fuel from fish processing industry waste in a diesel engine. *Clean Technol. Environ. Policy* **2017**, *19*, 1099–1108. [[CrossRef](#)]
3. Datta, A.; Mandal, B.K. An experimental investigation on the performance, combustion and emission characteristics of a variable compression ratio diesel engine using diesel and palm stearin methyl ester. *Clean Technol. Environ. Policy* **2017**, *19*, 1297–1312. [[CrossRef](#)]
4. Datta, A.; Mandal, B.K. A numerical study on the performance, combustion and emission parameters of a compression ignition engine fuelled with diesel, palm stearin biodiesel and alcohol blends. *Clean Technol. Environ. Policy* **2017**, *19*, 157–173. [[CrossRef](#)]
5. Chuah, L.F.; Aziz, A.R.A.; Yusup, S.; BokhariJir, A.; Klemes, J.; Abdullah, M.Z. Performance and emission of diesel engine fuelled by waste cooking oil methyl ester derived from palm olein using hydrodynamic cavitation. *Clean Technol. Environ. Policy* **2015**, *17*, 2229–2241. [[CrossRef](#)]
6. Kumar, B.R.; Saravanan, S. Effects of iso-butanol/diesel and n-pentanol/ diesel blends on performance and emissions of a DI diesel engine underpremixed LTC (low temperature combustion) mode. *Fuel* **2016**, *170*, 49–59. [[CrossRef](#)]
7. Basavarajshrigiri, M.; OmprakashHebbalb, D.; HemachandraReddya, K. Performance emission and combustion characteristics of semi, Adiabatic diesel engine using cotton seed and neem kernel oil methyl esters. *Alex. Eng. J.* **2016**, *55*, 699–706. [[CrossRef](#)]
8. Rakopoulos, D.; Rakopoulos, C.; Giakoumis, E.; Dimaratos, A.; Kyritsis, D. Effects of butanol–diesel fuel blends on the performance and emissions of a high-speed DI diesel engine. *Energy Convers. Manag.* **2010**, *51*, 1989–1997. [[CrossRef](#)]
9. Miers, S.; Carlson, R.; McConnell, S.; Ng, H.; Wallner, T.; Esper, J. *DriveCycle Analysis of Butanol/Diesel Blends in a Light-Duty Vehicle*; SAE Technical Paper Series, Article # 2008–01-2381; SAE: Warrendale, PA, USA, 2008. [[CrossRef](#)]
10. Karabektas, M.; Hosoz, M. Performance and emission characteristics of a dieselengine using isobutanol–diesel fuel blends. *Renew. Energy* **2009**, *34*, 1554–1559. [[CrossRef](#)]
11. Yao, M.; Wang, H.; Zheng, Z.; Yue, Y. Experimental study of n-butanol additive and multi-injection on HD diesel engine performance and emissions. *Fuel* **2010**, *89*, 2191–2201. [[CrossRef](#)]
12. Valentino, G.; Corcione, F.; Iannuzzi, S.; Serra, S. Experimental study on performance and emissions of a high speed diesel engine fuelled with n-butanol diesel blends under premixed low temperature combustion. *Fuel* **2012**, *92*, 295–307. [[CrossRef](#)]
13. Chen, Z.; Liu, J.; Han, Z.; Du, B.; Liu, Y.; Lee, C. Study on performance and emissions of a passenger-car diesel engine fueled with butanol–diesel blends. *Energy* **2013**, *55*, 638–646. [[CrossRef](#)]
14. Choi, B.; Jiang, X.; Kim, Y.; Jung, G.; Lee, C.; Choi, I.; Song, C. Effect of diesel fuelblend with n-butanol on the emission of a turbocharged common rail directinjection diesel engine. *Appl. Energy* **2015**, *146*, 20–28. [[CrossRef](#)]
15. Li, L.; Wang, J.; Wang, Z.; Liu, H. Combustion and emissions of compressionMignition in a direct injection diesel engine fueled with pentanol. *Energy* **2015**, *80*, 575–581. [[CrossRef](#)]

16. Li, L.; Wang, J.; Wang, Z.; Xiao, J. Combustion and emission characteristics of diesel engine fueled with diesel/biodiesel/pentanol fuel blends. *Fuel* **2015**, *156*, 211–218. [[CrossRef](#)]
17. Zhang, K.; Sawaya, M.; Eisenberg, D.; Liao, J. Expanding metabolism for biosynthesis of nonnatural alcohols. *Proc. Natl. Acad. Sci. USA* **2008**, *105*, 20653–20658. [[CrossRef](#)]
18. Dekishima, Y.; Lan, E.; Shen, C.; Cho, K.; Liao, J. Extending carbon chain length of 1-butanol pathway for 1-hexanol synthesis from glucose by engineered *Escherichia coli*. *J. Am. Chem. Soc.* **2011**, *133*, 11399–11401. [[CrossRef](#)]
19. Machado, H.B.; Dekishima, Y.; Luo, H.; Lan, E.I.; Liao, J.C. A selection platform for carbon chain elongation using the CoA-dependent pathway to produce linear higher alcohols. *Metab. Eng.* **2012**, *14*, 504–511. [[CrossRef](#)]
20. Verser, D. Method for the Indirect Production of Butanol and Hexanol. U.S. Patent 8252567 B2, Assignee to ZeeChem Inc., Menlo Park, CA, USA, 2012.
21. Ghaziaskar, H.; Xu, C. One-step continuous process for the production of 1-butanol and 1-hexanol by catalytic conversion of bio-ethanol at its sub-/supercritical state. *RSC Adv.* **2013**, *3*, 4271–4280. [[CrossRef](#)]
22. Phillips, J.; Atiyeh, H.; Tanner, R.; Torres, J.; Saxena, J.; Wilkins, M.; Huhnke, R. Butanol and hexanol production in *Clostridium carboxidivorans* syngas fermentation: Medium development and culture techniques. *Bioresour. Technol.* **2015**, *190*, 114–121. [[CrossRef](#)]
23. Venkatesan, E.P.; Murugesan, P.; Rajendran, S.; Sekar, P.; Remigios, P.A.; Chinna, R.B.D. Experimental Studies on Thermal-Barrier-Coated Engine Fuelled by a Blend of Eucalyptus Oil And DEE. *ACS Omega* **2022**, *50*, 46391–46401. [[CrossRef](#)] [[PubMed](#)]
24. Venkatesan, E.P.; Murugesan, P.; Ellappan, S.; Rajendran, S.; Aabid, A.; Abbas, M.; Saleel, C.A.; Remigios, P.A.; Reddy, M.S. Effect of Kariba Weed Biodiesel Blended with n-Pentane on the Chosen Parameters of a Ceramic-Coated Thermal Barrier Direct Injection Diesel Engine. *ACS Omega* **2022**, *50*, 46337–46346. [[CrossRef](#)] [[PubMed](#)]
25. Damodharan, D.; Sathiyagnanam, A.; Rana, D.; Kumar, B.R.; Saravanan, S. Extraction and characterization of waste plastic oil (WPO) with the effect of n-butanol addition on the performance and emissions of a DI diesel engine fueled with WPO/diesel blends. *Energy Convers. Manag.* **2017**, *131*, 117–126. [[CrossRef](#)]
26. Rajesh kumar, B.; Saravanan, S. Effect of exhaust gas recirculation (EGR) on performance and emissions of a constant speed DI diesel engine fueled with pentanol/diesel blends. *Fuel* **2015**, *160*, 217–226. [[CrossRef](#)]
27. Parthasarathy, M.; Elumalai, P.; Murunachippan, M.; Senthilkumar, P.; Shaik, S.; Sharifpur, M.; Khalilpoor, N. Influence of Injection Pressure on the Dual-Fuel Mode in CI Engines Fueled with Blends of Ethanol and Tamanu Biodiesel. *Int. J. Chem. Eng.* **2022**, *2022*, 6730963. [[CrossRef](#)]
28. Elumalai, P.; Balasubramanian, D.; Parthasarathy, M.; Pradeepkumar, A.; Iqbal, M.; Jayakar, J.; Nambiraj, M. An experimental study on harmful pollution reduction technique in low heat rejection engine fuelled with blends of pre-heated linseed oil and nano additive. *J. Clean. Prod.* **2021**, *283*, 124617. [[CrossRef](#)]
29. Nayak, S.K.; Hoang, A.T.; Nižetić, S.; Nguyen, X.P.; Le, T.H. Effects of advanced injection timing and inducted gaseous fuel on performance, combustion and emission characteristics of a diesel engine operated in dual-fuel mode. *Fuel* **2022**, *310*, 122232. [[CrossRef](#)]
30. Karthik, T.; Banapurmath, N.; Basavarajappa, D.; Ganachari, S.V.; Kulkarni, P.S.; Harari, P. Effect of injection timing on the performance of dual fuel engine fueled with algae nano-biodiesel blends and biogas. *Mater. Today Proc.* **2022**, *59*, 289–296. [[CrossRef](#)]
31. Kanth, S.; Debbarma, S.; Das, B. Experimental investigations on the effect of fuel injection parameters on diesel engine fuelled with biodiesel blend in diesel with hydrogen enrichment. *Int. J. Hydrog. Energy* **2022**, *47*, 35468–35483. [[CrossRef](#)]
32. Elumalai, P.V.; Parthasarathy, M.; Lalvani, J.S.C.I.J.R.; Mehboob, H.; Samuel, O.D.; Enweremadu, C.C.; Saleel, C.A.; Afzal, A. Effect of Injection Timing in Reducing the Harmful Pollutants Emitted from CI Engine Using N-Butanol Antioxidant Blended Eco-Friendly Mahua Biodiesel. *Energy Rep.* **2021**, *7*, 6205–6221. [[CrossRef](#)]
33. Verma, T.N.; Rajak, U.; Dasore, A.; Afzal, A.; Manokar, A.M.; Aabid, A. Experimental and empirical investigation of a CI engine fuelled with blends of diesel and roselle biodiesel. *Sci. Rep.* **2021**, *11*, 18865. [[CrossRef](#)] [[PubMed](#)]
34. Pinto, R.; Afzal, A.; D'Souza, L.; Ansari, Z.; Mohammed Samee, A.D. Computational Fluid Dynamics in Turbomachinery: A Review of State of the Art. *Arch. Comput. Methods Eng.* **2017**, *24*, 467–479. [[CrossRef](#)]
35. Afzal, A.; Ansari, Z.; Faizabadi, A.; Ramis, M. Parallelization Strategies for Computational Fluid Dynamics Software: State of the Art Review. *Arch. Comput. Methods Eng.* **2017**, *24*, 337–363. [[CrossRef](#)]
36. Afzal, A.; Aabid, A.; Khan, A.; Afghan, S.; Rajak, U.; Nath, T.; Kumar, R. Response Surface Analysis, Clustering, and Random Forest Regression of Pressure in Suddenly Expanded High-Speed Aerodynamic Flows. *Aerosp. Sci. Technol.* **2020**, *107*, 106318. [[CrossRef](#)]
37. Afzal, A.; Nawfal, I.; Mahbulul, I.M.; Kumbar, S.S. An Overview on the Effect of Ultrasonication Duration on Different Properties of Nanofluids. *J. Therm. Anal. Calorim.* **2019**, *135*, 393–418. [[CrossRef](#)]
38. Doğan, O. The influence of n-butanol/diesel fuel blends utilization on a small diesel engine performance and emissions. *Fuel* **2011**, *90*, 2467–2472. [[CrossRef](#)]
39. Afzal, A.; Abdul Mujeebu, M. Thermo-Mechanical and Structural Performances of Automobile Disc Brakes: A Review of Numerical and Experimental Studies. *Arch. Comput. Methods Eng.* **2019**, *26*, 1489–1513. [[CrossRef](#)]
40. Jilte, R.; Afzal, A.; Panchal, S. A Novel Battery Thermal Management System Using Nano-Enhanced Phase Change Materials. *Energy* **2021**, *219*, 119564. [[CrossRef](#)]

41. Asif, A.; Khan, S.A.; Salee, C.A. Role of Ultrasonication Duration and Surfactant on Characteristics of ZnO and CuO Nanofluids. *Mater. Res. Express* **2019**, *6*, 1150d8. [[CrossRef](#)]
42. Samyalingam, L.; Aslfattahi, N.; Saidur, R.; Mohd, S.; Afzal, A. Solar Energy Materials and Solar Cells Thermal and Energy Performance Improvement of Hybrid PV/T System by Using Olein Palm Oil with MXene as a New Class of Heat Transfer Fluid. *Sol. Energy Mater. Sol. Cells* **2020**, *218*, 110754. [[CrossRef](#)]
43. Afzal, A.; Alshahrani, S.; Alrobaian, A.; Buradi, A.; Khan, S.A. Power Plant Energy Predictions Based on Thermal Factors Using Ridge and Support Vector Regressor Algorithms. *Energies* **2021**, *14*, 7254. [[CrossRef](#)]
44. Said, Z.; Sharma, P.; Syam Sundar, L.; Afzal, A.; Li, C. Synthesis, Stability, Thermophysical Properties and AI Approach for Predictive Modelling of Fe<sub>3</sub>O<sub>4</sub> Coated MWCNT Hybrid Nanofluids. *J. Mol. Liq.* **2021**, *340*, 117291. [[CrossRef](#)]
45. Afzal, A.; Samee, A.D.M.; Jilte, R.D.; Islam, T.; Manokar, A.M.; Abdul, K. Battery Thermal Management: An Optimization Study of Parallelized Conjugate Numerical Analysis Using Cuckoo Search and Artificial Bee Colony Algorithm. *Int. J. Heat Mass Transf.* **2021**, *166*, 120798. [[CrossRef](#)]
46. Afzal, A.; Mohammed Samee, A.D.; Abdul Razak, R.K.; Ramis, M.K. Effect of Spacing on Thermal Performance Characteristics of Li-Ion Battery Cells. *J. Therm. Anal. Calorim.* **2019**, *135*, 1797–1811. [[CrossRef](#)]
47. Afzal, A.; Navid, K.M.Y.; Saidur, R.; Razak, R.K.A.; Subbiah, R. Back Propagation Modeling of Shear Stress and Viscosity of Aqueous Ionic—MXene Nanofluids. *J. Therm. Anal. Calorim.* **2021**, *145*, 2129–2149. [[CrossRef](#)]
48. Yunus Khan, T.M.; Soudagar, M.E.M.; Kanchan, M.; Afzal, A.; Banapurmath, N.R.; Akram, N.; Mane, S.D.; Shahapurkar, K. Optimum Location and Influence of Tilt Angle on Performance of Solar PV Panels. *J. Therm. Anal. Calorim.* **2019**, *141*, 511–532. [[CrossRef](#)]
49. Afzal, A.; Ramis, M.K. Multi-Objective Optimization of Thermal Performance in Battery System Using Genetic and Particle Swarm Algorithm Combined with Fuzzy Logics. *J. Energy Storage* **2020**, *32*, 101815. [[CrossRef](#)]
50. Mokashi, I.; Afzal, A.; Khan, S.A.; Abdullah, N.A.; Bin Azami, M.H.; Jilte, R.D.; Samuel, O.D. Nusselt Number Analysis from a Battery Pack Cooled by Different Fluids and Multiple Back-Propagation Modelling Using Feed-Forward Networks. *Int. J. Therm. Sci.* **2021**, *161*, 106738. [[CrossRef](#)]
51. Soudagar, M.E.M.; Kalam, M.A.; Sajid, M.U.; Afzal, A.; Banapurmath, N.R.; Akram, N.; Mane, S.D.; Saleel C, A. Thermal Analyses of Minichannels and Use of Mathematical and Numerical Models. *Numer. Heat Transf. Part A Appl.* **2020**, *77*, 497–537. [[CrossRef](#)]
52. Afzal, A.; Samee, M.; Ahmed Kaladgi, A.R. Experimental Thermal Investigation of CuO-W Nanofluid in Circular Minichannel. *Model. Meas. Control B* **2017**, *86*, 335–344. [[CrossRef](#)]
53. Afzal, A.; Samee, A.D.M.; Razak, R.K.A.; Ramis, M.K. Heat Transfer Characteristics of MWCNT Nanofluid in Rectangular Mini Channels. *Int. J. Heat Technol.* **2018**, *36*, 222–228. [[CrossRef](#)]
54. Tamilselvi, S.; Gunasundari, S.; Karuppiyah, N.; Razak Rk, A.; Madhusudan, S.; Nagarajan, V.M.; Sathish, T.; Shamim, M.Z.M.; Saleel, C.A.; Afzal, A. A Review on Battery Modelling Techniques. *Sustainability* **2021**, *13*, 10042. [[CrossRef](#)]
55. Hochreiter, S.; Schmidhuber, J. Long Short-Term Memory. *Neural Comput.* **1997**, *9*, 1735–1780. [[CrossRef](#)] [[PubMed](#)]
56. Pichika, N.; Meganaa, G.; Rajasekharan, S.G.; Malapati, A. Multi-component fault classification of a wind turbine gearbox using integrated condition monitoring and hybrid ensemble method approach. *Appl. Acoust.* **2022**, *195*, 108814. [[CrossRef](#)]
57. Pichika, N.; Yadav, R.; Rajasekharan, S.G.; Praveen, H.M.; Inturi, V. Optimal sensor placement for identifying multi-component failures in a wind turbine gearbox using integrated condition monitoring scheme. *Appl. Acoust.* **2022**, *187*, 108505. [[CrossRef](#)]

**Disclaimer/Publisher’s Note:** The statements, opinions and data contained in all publications are solely those of the individual author(s) and contributor(s) and not of MDPI and/or the editor(s). MDPI and/or the editor(s) disclaim responsibility for any injury to people or property resulting from any ideas, methods, instructions or products referred to in the content.